ICC
Iranian Chemical Communication
Original Research Article
Payame Noor University http://icc.journals.pnu.ac.ir

A study on the comparison between thermodynamics and kinetics of reaction of the ozone and mercury, silver and gold

Vahid Moeini*, Seyed Hojatollah Rahimi, Zohre Rakhsha

[a]*Department of Chemistry, Payame Noor University, P.O. BOX 19395-3697, Tehran, Iran*

Received: 11 June 2014, Accepted: 4 September 2015, Published: 5 September 2015

Abstract

In this work, we report results of calculations based on the density functional theory of different species of metal-ozone, containing mercury, silver and gold. The chosen species range from small molecules and large transition-metals containing ozone with mercury, silver and gold complexes. A comparative analysis of the description of the metal-oxygen bond obtained by different methodologies is presented. The topology of the electronic density of the metal-ozone is studied, at DFT level, using the theory of atoms in molecules (AIM) developed by Bader. Thermodynamic variables of reactions have been calculated. The effect of temperature on thermodynamics quantities of the reaction has also been investigated. The LanL2MB basis set for mercury, silver and gold with ozone are used at the B3LYP method. The energy levels of the HOMO and LUMO orbitals compute at the B3LYP/LanL2MB level.

Keywords: density functional theory; transition state; ozone; mercury; silver; gold.

Introduction

The ozone layer is a protective shield that blocks the sun's harmful ultraviolet rays from reaching the earth's surface. However, the ozone layer is destroyed by chemical componds known as ozone-depleting substances. Scientific research has proved that the natural balance of stratospheric ozone has been damaged by the production and release of ozone-depleting substances, including chlorofluorocarbons (CFC), halons, methyl chloroform, carbon tetrachloride,

*Corresponding author: Vahid Moeini
Tel: +98 (11) 34646231, Fax: +98 (11) 34646833
E-mail: v_moeini@yahoo.com

hydrochlorofluorocarbons (HCFCs) and methyl bromide. These substances are found in refrigerators, air conditioners, fire extinguishers, aerosols, agricultural fumigants, foam and in solvents for cleaning electronic equipment. Atomic oxygen plays an important part in the formation of atmospheric ozone. Oxygen atoms form in the dissociation of an O2 molecule either associate again in the presence of another particle necessary to withdraw the energy from a form molecule according to the equation or interact with an O_2 molecule also in the presence of another particle and form of an ozone molecule as follows. Physically, an ozone molecule is stable, but the decomposition rate of gaseous ozone grows appreciably with an increase in the temperature and amounts of some gases, and also under the action of different radiations and particle fluxes [1, 2].

Mercury remains in use in scientific research applications and in amalgam material for dental restoration in some locales. It is used in lighting, electricity passed through mercury vapor in a fluorescent lamp produces short-wave ultraviolet light which then causes the phosphor in the tube to fluoresce, making visible light. Silver metal is used industrially in electrical contacts and conductors, in mirrors and in catalysis of chemical reactions. Gold has been a valuable and highly sought-after precious metal for coinage, jewelry, and other arts since long before the beginning of recorded history. [3-7].

Density functional theory (DFT) describes the electronic states of atoms, molecules, and materials and also it can be a preferred method for electronic structure theory for complex chemical systems, in part yet it competes well in accuracy except for very small systems. This is true even in organic chemistry, but the advantages of DFT are still greater for metals, especially transition metals. The reason for this added advantage is static electron correlation. It is now well appreciated that quantitatively accurate electronic structure calculations must include electron correlation. It is convenient to recognize two types of electron correlation, the first called dynamical electron correlation and the second called static correlation, near-degeneracy correlation, or nondynamical correlation. Dynamical correlation is a short-range effect by which electrons avoid one another to reduce electron repulsion. It is a very general effect for all finite systems containing two or more electrons [8-10]. Accounting for dynamical correlation by a configuration

interaction wave function is very slowly convergent and requires a very large number of configurations. Other correlation effects, which are very system specific and can be either medium ranged or long ranged, can be accounted for to a large extent by mixing a small number sometimes two, sometimes more of configurations that are ‘‘nearly’’ degenerate. In this work, we consider the subject of reaction of the ozone’s molecules with mercury, silver and gold metals by DFT. We selected recent paper that Section 2 reviews the computational method; section 3 contains some result and discussion, and reviews validation studies by thermochemistry. Section 4 reviews molecular orbital analysis and section 5 contains concluding remarks.

Computational

Method used

The optimized geometries of reactants, products, complexes in two possible transition states (TS), cyclic (TS1) and non cyclic (TS2) obtain using the density functional theory with Becke 3-parameter hybrid exchange and Lee – Yong - Parr correlation (B3LYP) calculations that have been shown in Figure 1.

Figure 1. The optimized geometries of the complexes of two possible transition states cyclic (TS1) and non cyclic (TS2) at B3LYP/ LanL2MB level

The LanL2MB basis set for mercury, silver and gold with ozone are used at the B3LYP method (Table 1) [11-13]. This work has been also repeated by the Moller-Plesset many-body perturbation theory method to second order (MP2) using LanL2DZ basis set (Table 2).

Table 1. Total energy (au) values of the structures considered for all species of mercury, silver and gold with ozone reaction in B3LYP/ LanL2MB level

Reactions	**Total energy**	**Corrected total energy**	**BSSE**
Hg (g) + O_3	-265.1268	-265.1194	
$TS1_{Hg}$	-265.1615	-265.1527	0.0312
$TS2_{Hg}$	-265.1440	-265.1361	0.0224
HgO(g) + O_2	-264.9874	-264.9824	
Ag (g) + O_3	-368.1021	-368.0947	
$TS1_{Ag}$	-368.1738	-368.1670	
$TS2_{Ag}$	-368.1563	-368.1488	
AgO(g) + O_2	-368.0451	-368.0405	
Au (g) + O_3	-357.7843	-359.7769	
$TS1_{Au}$	-357.8390	-357.8306	
$TS2_{Au}$	-357.8560	-357.8484	
AuO(g) + O2	-357.7476	-357.7427	

Table 2. Total energy (au) values of the structures considered for all species of mercury, silver and gold with ozone reaction in MP2/LanL2DZ level

Reactions	**Total energy**	**Corrected total energy**	**BSSE**
Hg (g) + O_3	-266.1651	-266.1535	
$TS1_{Hg}$	-266.1819	-266.1702	**0.0076**
$TS2_{Hg}$	-266.1675	-266.1557	**0.0027**
HgO(g) + O_2	-266.1019	-266.0995	
Ag (g) + O_3	-369.6341	-369.6225	
$TS1_{Ag}$	-369.5180	-369.2538	
$TS2_{Ag}$	-369.6535	-369.6529	
AgO(g) + O_2	-369.6428	-369.6404	
Au (g) + O_3	-359.2554	-359.2438	
$TS1_{Au}$	-359.2638	-359.2538	

$TS2_{Au}$	-359.2541	-359.2418
AuO(g) + O2	-359.1269	-359.1243

Transition states, zero point energies (ZPE) and thermodynamic contributions to the gaseous phase at T = 298.15 K and atmospheric pressure for optimized structures were calculated at the same levels of theory. The quantities that have been deduced for these metals are given in Tables 3 to 5.

Table 3. Relative internal energies, enthalpies, free energies, and $T\Delta S$ (kcal.mol^{-1}) for steps of reactions with ZPE correction for mercury

Reactions	**Δ*E***	**Δ*H***	***TΔS***	**Δ*G***
B3LYP/LanL2MB				
$Hg(g)+O_3(g) \rightarrow TS1$	-20.77	-21.4	-7.41	-13.99
$TS1 \rightarrow TS2$	10.92	10.85	1.88	8.97
$TS2 \rightarrow HgO(g)+O_2$	96.13	96.76	6.65	90.11
$Hg(g)+O_3(g) \rightarrow HgO(g)+O_2(g)$	86.28	86.22	1.19	85.03
MP2/LanL2DZ				
$Hg(g)+O_3(g) \rightarrow TS1$	-10.23	-10.79	-6.64	-3.95
$TS1 \rightarrow TS2$	9.04	8.97	0.94	8.03
$TS2 \rightarrow HgO(g)+O_2$	35.52	36.14	7.52	28.62
$Hg(g)+O_3(g) \rightarrow HgO(g)+O_2(g)$	34.32	34.32	1.56	32.76

Table 4. Relative internal energies, enthalpies, free energies, and $T\Delta S$ (kcal.mol^{-1}) for steps of reactions with ZPE correction for silver

Reaction	**Δ*E***	**Δ*H***	***TΔS***	**Δ*G***
B3LYP/LanL2MB				
$Ag(g)+O_3(g) \rightarrow TS1$	-45.94	-46.12	-8.09	-38.03
$TS1 \rightarrow TS2$	11.42	11.42	0.00	11.42

$TS2 \rightarrow AgO(g)+O_2$	68.52	69.15	9.54	59.61
$Ag(g)+O_3(g) \rightarrow AgO(g)+O_2(g)$	34.45	34.45	1.45	33.00
MP2/LanL2DZ				
$Ag(g)+O_3(g) \rightarrow TS1$	2.38	3.01	-8.79	76.56
$TS1 \rightarrow TS2$	9.04	8.97	0.94	-6.78
$TS2 \rightarrow AgO(g)+O_2$	-81.51	-81.58	0.69	-82.27
$Ag(g)+O_3(g) \rightarrow AgO(g)+O_2(g)$	-10.86	-10.79	1.70	-12.49

Table 5. Relative internal energies, enthalpies, free energies, and $T\Delta S$ (kcal.mol^{-1}) for steps of reactions with ZPE correction for gold

Reaction	**ΔE**	**ΔH**	**$T\Delta S$**	**ΔG**
B3LYP/LanL2MB				
$Au(g)+O_3(g) \rightarrow TS1$	-33.38	-33.95	-7.09	-26.86
$TS1 \rightarrow TS2$	-11.61	-11.67	-1.19	-10.48
$TS2 \rightarrow AuO(g)+O_2$	66.77	67.46	9.54	57.92
$Au(g)+O_3(g) \rightarrow AuO(g)+O_2(g)$	21.77	21.84	1.20	20.64
MP2/LanL2DZ				
$Au(g)+O_3(g) \rightarrow TS1$	-6.15	-6.71	-7.46	0.753
$TS1 \rightarrow TS2$	7.15	7.15	-0.94	8.09
$TS2 \rightarrow AuO(g)+O_2$	73.98	74.92	9.91	65.01
$Au(g)+O_3(g) \rightarrow AuO(g)+O_2(g)$	74.99	75.36	1.50	73.86

Additionally to confirm the optimized structures of all species the topological analyses of atoms in molecules (AIM) were carried out by means of the AIM2000 series of programs. All calculations were performed using the quantum chemical software GAUSSIAN 09 [14-16]. Comparison of calculation results for some studied molecules with experimental values suggested that the most reliable geometries are obtained at B3LYP level, so these were utilized in the final analysis with respect to

the energies [17]. Because of the lower level of transition states energies results, it is expected to be more reliable, so they are given in tables for comparison. The AIM calculated results of transition states are shown in Figure 2 and Table 6.

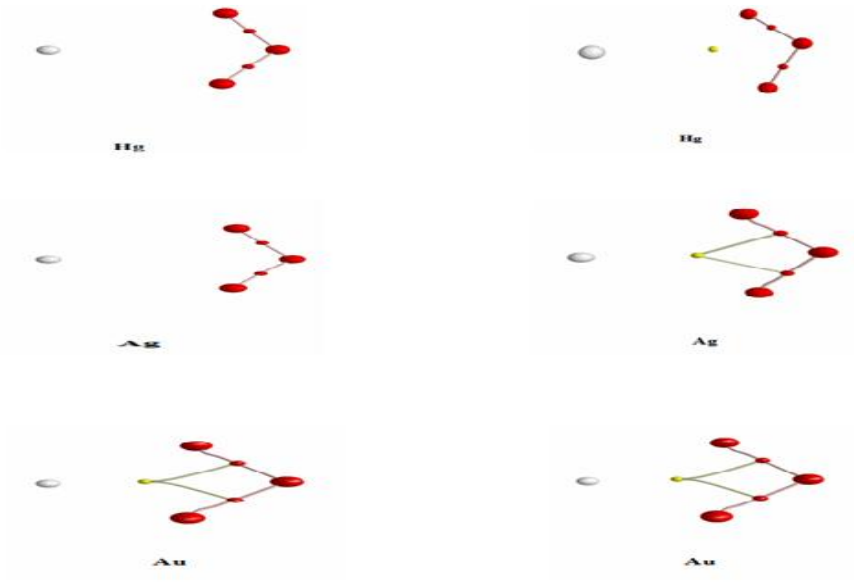

Figure 2. Molecular structure of the transition states TS1 (right), TS2 (left), showing the bond paths and the bond (small red circles) and ring (small yellow circles) critical points

Table 6. Topological parameters (in au), the electron densities $\rho(r)$; at metal-O_3 RCPs, their Laplacians $\nabla^2\rho$ and energetic parameters $V(r)$, $G(r)$ and $H(r)$ in parentheses refer to aqueous solution.

	$\rho(r)$	$\nabla^2\rho$	$G(r)$	$V(r)$	$H(r)$
$TS1_{Hg}$, Hg-O_3	0.0141	0.0812	0.0171	-0.014	0.0031
$TS1_{Ag}$, Ag-O_3	0.0188	0.1244	0.0267	-0.0223	0.0044
$TS1_{Au}$, Au-O_3	0.0209(0.022)	0.1368(0.148)	0.0295(0.0327)	-0.0248(-0.0282)	0.0047(0.0045)

Results and discussion

Elemental mercury, silver, gold and their reactions with atmospheric species have been studied by using both the density functional theory and the Moller-Plesset many-body perturbation theory method to second order (MP2). The effect of aqueous solvent has been studied using the effect of water molecule with complex of ozone-mercury, ozone-silver and ozone-gold reactions. Reaction of ozone with mercury, silver and gold is possible from doublet pathway. Based

on our calculated results, the first step of reaction is formation of a cyclic transition states complex (TS1). Other step of reaction is formation of a non cyclic transition states complex (TS2). The geometric parameters of transition states complexes involved in reactions are schematized in Figure 3.

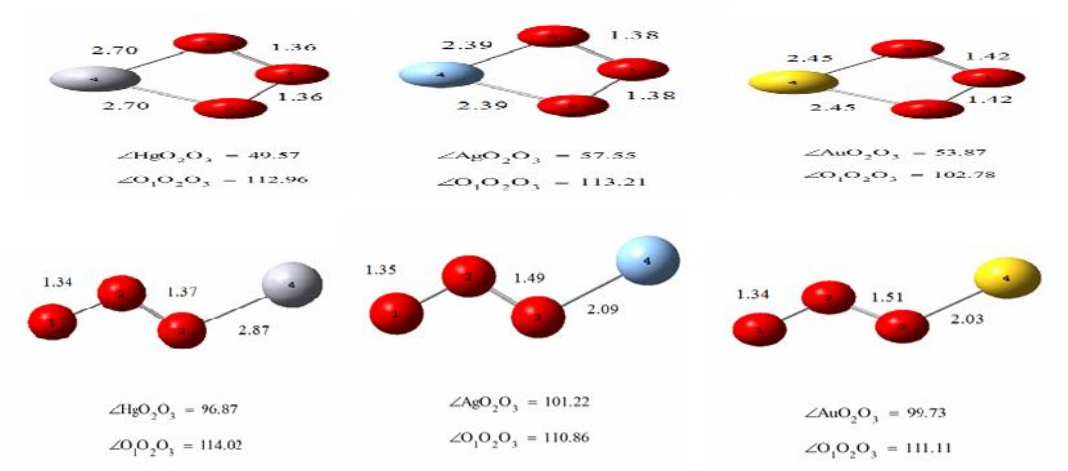

Figure 3. Structural parameters of transition species of gaseous medium in B3LYP/lanl2mb level of theory. Bond lengths are on angstrom and bond angle in degrees in reaction of ozone with mercury, silver and gold.

All of species and pathways confirm using theoretical results such as geometry optimization, the total energies, AIM topological and thermochemistry of pathways that are obtained. Comparison of TS of metals by the free energy of activation show that metal of Hg with ozone molecules are formed cyclic and non cyclic complexes for low and high temperatures, respectively. But, Au metal shows reverse condition, because complex of this metal with ozone molecule is cyclic at low temperature that with temperature increasing is converted to non cyclic complex, and Ag metal with ozone molecule show cyclic complex in this temperature range. The results show that the complexes of metals can turn to the HgO, AgO, AuO and O2. The geometric parameters of all species involved in the reaction (TS1Hg, TS1Ag, TS1Au, TS2Hg, TS2Ag, TS2Au and O3) are calculated and compared in some cases with the available corresponding experimental data or other theoretical results. Several excellent reviews which have been published on the theory of atoms in molecules (AIM) developed by other authors have been based on the critical points of the molecular electronic charge

density, $\circ(r)$. Four types of critical points are of interest in molecules. One of them is the bond between critical points, which corresponds to a maximum in $\circ(r)$ characterized by $\nabla^2\circ$ and occurs between two neighboring nuclei, indicating the existence of a bond between them. Another one is the ring critical points that indicate the formation of a ring between three or more atoms [17-20]. AIM has been shown to provide valuable information about many different chemical systems by an analysis of molecular ozone-mercury, ozone-silver and ozone-gold reactions. The positive value of Laplacian, $\nabla^2\circ$ according to the bond critical points indicates weak intermolecular or ionic bond and the negative value of Laplacian shows the strong covalent bonds between the atoms. The absolute value of Laplacian and the bond critical points value is related to the bond order between two neighboring nuclei. The values of bond critical points parameters and electronic density gradient satisfy criteria for some important bonds. Thus, it shows the positions of the maxima in electron density and bond paths connecting the nuclei, as well as the positions of the bond critical points and ring critical points. But, two topological parameters, the Laplacian $\nabla^2\circ$ and the total energy density $H(r)$ at BCP are often applied to classify and characterize metal oxygen bonds. The ring critical points are appear in systems which the bond paths form a ring. They are located in the interior of the rings and are defined by the termini of all trajectories $\nabla\circ$ coming from infinity and going to the bond critical points and to the attractors. The $\nabla\circ$ trajectories linking the attractors and bond critical points that the ring contains form the so called ring surfaces. In this work, molecular graphs (set of bond paths and critical points) of the three complexes defined in figure 2, the region of interest showing the bay region ring involving the three oxygen atoms with metal atom. Color code for critical points are small spheres, bond critical points (BCPs, red) and ring critical points (RCPs, yellow) [20, 21].

The change of thermodynamic properties for every reaction is also calculated from the corresponding thermodynamic properties of products and reactants. Their value is corrected by zero point energy (ZPE) for the reaction. The calculated free energy of activation for cyclic and non cyclic transition state has been also calculated for various temperatures have been summarized in Tables 7 and 8.

Table 7. The free energy of activation (kcal.mol^{-1}) for cyclic transition state (TS1) in gaseous medium compared at various temperatures

***T*/K**	$\Delta^{\pm}G_{TS1Hg}$	$\Delta^{\pm}G_{TS1Ag}$	$\Delta^{\pm}G_{TS1Au}$
100	-16.91	-35.71	-29.64
500	-9.83	-33.28	-22.88
1000	1.42	-20.28	-12.19
1500	12.42	-7.14	-1.80
2000	23.25	6.13	8.50
2500	33.96	19.51	18.64
3000	44.56	32.99	28.68

Table 8. The free energy of activation (kcal.mol^{-1}) for non cyclic transition state (TS2) in gaseous medium compared at various temperatures

***T*/K**	$\Delta^{\pm}G_{TS2Hg}$	$\Delta^{\pm}G_{TS2Ag}$	$\Delta^{\pm}G_{TS2Au}$
100	-8.90	-24.27	-42.86
500	-2.21	-21.87	-32.46
1000	5.70	-8.79	-19.00
1500	13.35	4.51	-5.325
2000	20.83	17.96	8.50
2500	28.18	31.52	22.44
3000	35.43	45.18	36.48

The data of Tables 9 and 10 have been also shown by a logarithmic k versus $1/T$ plot in Figures 4 and 5 for cyclic and non cyclic transition state at various temperatures, respectively [17].

Table 9. Comparison between rate constants logarithm as a function of temperature for cyclic transition state of mercury, silver and gold elements and ozone molecule in gaseous medium

T/K	$\mathbf{Ln}k_{TS1Hg}$	$\mathbf{Ln}k_{TS1Ag}$	$\mathbf{Ln}k_{TS1Au}$
100	114.56	209.18	178.63

500	39.35	62.96	51.49
1000	30.17	39.67	35.59
1500	25.29	31.85	30.06
2000	23.61	27.96	27.32
2500	22.66	24.55	25.71
3000	17.35	23.93	24.65

Table 10. Comparison between rate constants logarithm as a function of temperature for non cyclic transition state of mercury, silver and gold elements and ozone molecule in gaseous medium

T/K	**Lnk_{TS2Hg}**	**Lnk_{TS2Ag}**	**Lnk_{TS2Au}**
100	74.26	151.62	245.14
500	31.68	51.47	62.12
1000	26.59	33.88	39.02
1500	24.98	27.94	31.242
2000	24.22	24.94	27.32
2500	23.78	23.11	24.94
3000	23.51	21.89	23.34

In these cases, rates of reaction decrease with increasing temperature. When following an approximately exponential relationship the constant rate can be fit to an Arrhenius expression, this results in a negative value of E_a. Elementary reactions exhibiting these negative activation energies are typically barrierless reactions, in which the reaction proceeding relies on the capture of the molecules in a potential well. Increasing the temperature leads to a reduced probability of the colliding molecules capturing one another (with more glancing collisions not leading to reaction as the higher momentum carries the colliding particles out of the potential well), expressed as a reaction cross section that decreases with increasing temperature. Such a situation no longer leads to direct interpretations as the height of a potential spot. A large number of reactions of the type $\dot{R} + HX$ and $\dot{R} + X_2$ have been reported as having negative activation energies where X

is I, Br, Cl. These reactions have none of the behavior of reactions that are expected to have negative activation energies. It is shown that they must be simple metathesis reactions having a single transition state. Some of what appear to be simple metathesis reactions but proceed *via* atom plus radical recombination has had rate constants reported, close to the collision limit [22, 23].

In this paper, accordingly, the expected rate constant value at each temperature, the values of ln *k* plotted against 1/*T* (Arrhenius plot) have been shown in Figures 4 and 5 for cyclic and non cyclic transition state at various temperatures, respectively. Data on ln *k* vs 1/*T* can be fitted to the Arrhenius equation, yielding negative and apparently constant values of activation energy *E*a.

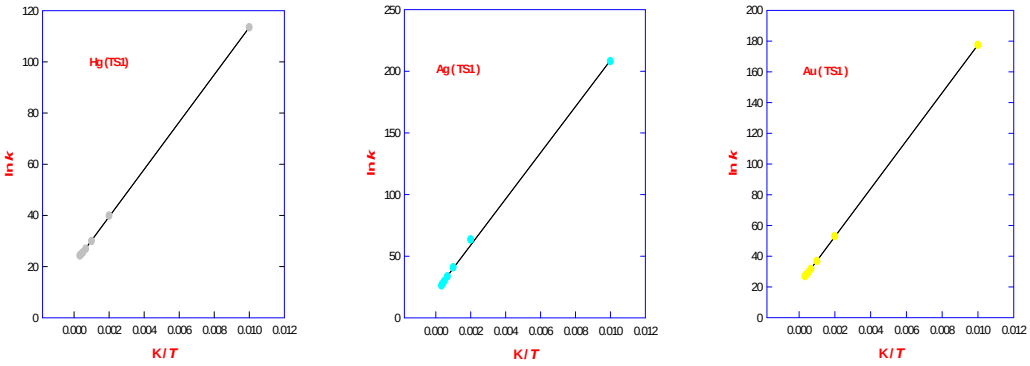

Figure 4. The Arrhenius plot for mercury, silver and gold with ozone in gaseous medium (cyclic TS1)

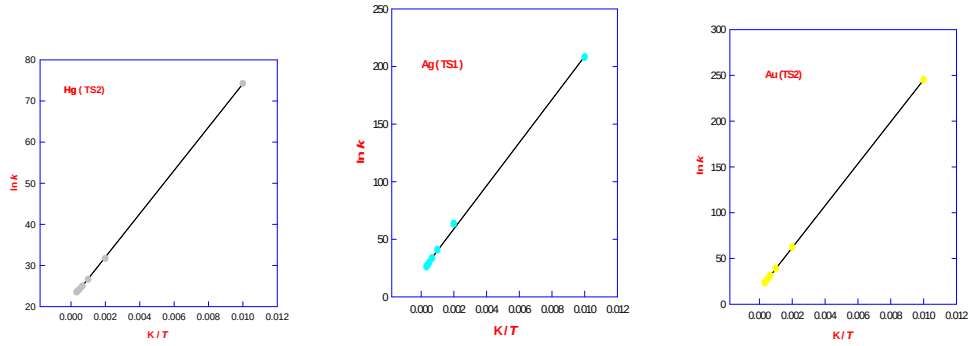

Figure 5. The Arrhenius plot for mercury, silver and gold with ozone in gaseous medium (non cyclic TS2)

The relative free energy values for these reactions over the temperature range 100 to 3000 K are presented in Table 11. The variations of the relative free energies with

temperature at the different temperatures have been shown in Figures 6. From analysis of the data, it was found that the relative free energies depend more strongly on the temperature of reaction.

Table 11. ΔG values (kcal.mol^{-1}) of the structures considered B3LYP/LanL2MB (aqueous medium in parenthesis)

***T*/K**	**100**	**500**	**1000**	**1500**	**2000**	**2500**	**3000**
ΔG_{ReHg}	85.65(70.21)	83.46(68.61)	80.63(66.44)	77.94(64.63)	75.36(62.56)	72.92(60.81)	70.66(59.15)
ΔG_{ReAg}	41.42(31.48)	31.19(29.63)	27.86(27.02)	24.66(24.56)	21.59(22.23)	18.64(20.02)	15.75(17.90)
ΔG_{ReAu}	21.21(19.40)	19.01(17.83)	16.13(15.68)	13.43(13.68)	8.97(11.84)	8.35(10.10)	6.02(8.46)

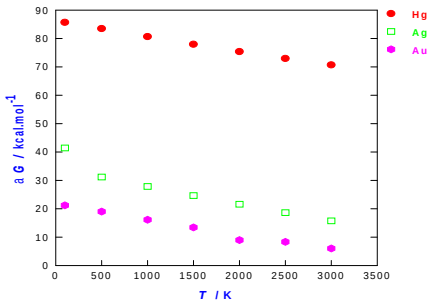

Figure 6. The ΔG / kcal.mol^{-1} of the reactions of mercury, silver and gold with ozone molecule as a function of temperature

Molecular orbital analysis

The highest occupied molecular orbital (HOMO) and the lowest lying unoccupied molecular orbital (LUMO) are named as frontier molecular orbitals (FMO). A molecule with a small frontier orbital gap is more polarizable and is generally associated with a high chemical reactivity and low kinetic stability and is also termed as soft molecule. The HOMO-LUMO energy gap of a molecule will play a crucial role in deciding its bioactive properties and is a very important parameter for quantum chemistry [24]. The HOMO energy distinguishes the capacity of electron donor, whereas LUMO energy characterizes the capacity of electron acceptor, and the gap distinguishes the chemical stability. The distributions and energy levels of the HOMO and LUMO orbitals computed at the B3LYP/LanL2MB level for the cyclic and non cyclic complexes have been shown in Figure 7.

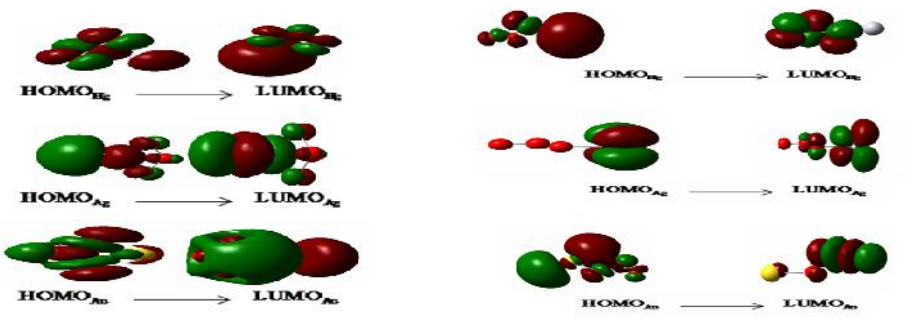

Figure 7. The HOMO and LUMO cyclic (left) and non cyclic (right) complexes of mercury, silver and gold with ozone in gaseous medium

The calculations indicate that the cyclic complex has the value of the energy separation between the HOMO and LUMO which are −0.175 and −0.096 eV for Hg, −0.163 and −0.061 eV for Ag and −0.203 and −0.099 eV for Au at the same levels, respectively. The non cyclic complexes also show the energy separation between the HOMO and LUMO -0.165 and -0.139 eV for Hg, -0.155 and -0.104 eV for Ag and -0.184 and -0.123 eV for Au at the same levels, respectively. Tables 12 and 13 show the HOMO, LUMO, and the interfrontier molecular orbital energy gap (Δ*E*) values of the species for cyclic and non cyclic complexes, respectively. The change of thermodynamic property for various reaction channels are the difference between the thermodynamics data of product from reactant.

Table 12. The HOMO and LUMO energies (eV) and interfrontier energy gaps (Δ*E*) of the cyclic complexes structure considered in gaseous medium

Orbital molecular energy	**$TS1_{Hg}$**	**$TS1_{Ag}$**	**$TS1_{Au}$**
E(HOMO)	-0.175	-0.163	-0.203
E(LUMO)	-0.096	-0.061	-0.099
Δ*E*(HOMO-LUMO)	-0.079	-0.102	-0.104

Table 13. The HOMO and LUMO energies (eV) and interfrontier energy gaps (ΔE) of the non cyclic complexes structure considered in gaseous medium

Orbital molecular energy	**$TS2_{Hg}$**	**$TS2_{Ag}$**	**$TS2_{Au}$**
E(HOMO)	-0.165	-0.155	-0.184
E(LUMO)	-0.139	-0.104	-0.123
ΔE(HOMO-LUMO)	-0.026	-0.051	-0.061

Au and Ag are characterized with the lowest and highest lying HOMO energy values, respectively. Irrespective of the complexes structure used, the order is $AgO_3 \succ HgO_3 \succ AuO_3$, whereas the order of LUMO energies for cyclic complexes structure is $AgO_3 \succ HgO_3 \succ AuO_3$ and for noncyclic complexes structure is $AgO_3 \succ AuO_3 \succ HgO_3$.

Conclusion

In order to test the performance of the computational method, we compare these efficiently calculated DFT results with the highly accurate but computationally expensive post-Hartree-Fock approaches of Moler-Plesset second-order many body perturbation theory (MP2). The calculations are carried out as implemented in Gaussian 09 Package. The relativistic effective core pseudo potentials (LANL2DZ) and the experimental basis sets are employed in the studies of the relativistic partially bonding between metal-oxygen in complexes mercury, silver and gold with ozone molecules. In other words, consideration of atomic mercury, silver and gold reactions with ozone molecules, geometry optimization and AIM analysis of all components of reaction have been used for confirmation of reaction mechanism. Thermodynamic variable of all reactions have been calculated and also the results for the Gibbs free energy of reactions at different temperatures are listed in table 6. According to the results of calculations, the most favorable change is $Au + O_3 \rightarrow AuO + O_2$ and then $Ag + O_3 \rightarrow AgO + O_2$, whereas the least likely one among the mentioned reactions is $Hg + O_3 \rightarrow HgO + O_2$. Also the Gibbs free energy of reactions at different temperatures show that the reactions favorability increases with temperature decreasing.

Acknowledgements

The authors thank Payame Noor University for the financial support.

References

[1] S.S. Yelisetty, D.P. Visco, *J. Chem. Eng. Data*, **2009**, *54*, 781–785.

[2] H. Roohi, E. Ahmadepour, *Phys. Chem. Res*., **2013**, *1*, 41-51.

[3] D.R. Canant, H.S. Swofford, Jr. *J. Chem. Eng. Data* **1969**, *14*, 369–372.

[4] H.K. Yuan, A.L. Kuang, C.L. Tian, H. Chen, *AIP Advances*, **2014**, *4*, 037107.

[5] E. Kraisler, L. Kronic, *J. Chem. Phys.*, **2014**, *140*, 18A540.

[6] A. Mirtschink, C.J. Umrigar, J.D. Morgan lll, P. Gori-Giorgi, *J. Chem. Phys.*, **2014**, *140*, 18A532.

[7] M.C. Kim, E. Sim, K. Burke, *J. Chem. Phys.*, **2014**, *140*, 18A528.

[8] A. Beche, *J. Chem. Phys.*, **2014**, *140*, 18A301.

[9] E.C. Bushnell, T. Burns, R. Boyd, *J. Chem. Phys.*, **2014**, *140*, 18A519.

[10] T. Tsuneda, K. Hirao, *J. Chem. Phys.*, **2014**, *140*, 18A513.

[11] T. Schimdt, E. Kraisler, A. Makmal, L. Kronik, S. Kummel, *J. Chem. Phys.*, **2014**, *140*, 18A510.

[12] A. Ambrosetti, A.M. Reilly, R.A. DiStasio Jr., A. Tkatchenko, *J. Chem. Phys.*, **2014**, *140*, 18A508.

[13] J. Goodpaster, T.Barnes, F. Manby, T. Miller lll, *J. Chem. Phys.*, **2014**, *140*, 18A507

[14] M.J.S. Dewar, C. H. Reynolds, *J. Comp. Chem.*, **1986**, *2*,140.

[15] M.J. Frisch et al, Gaussian 03, Revision B.03, **2003**, Gaussian, Inc.: Pittsburgh, PA.

[16] J.B. Foresman, AE. Frisch, Exploring Chemistry with Electronic Structure Methods: A Guide Using *Gaussian*, August **1996**.

[17] M. Vahedpour, M. Tozihi, F. Nazari, *Journal of the Chinese Chemical Society*, **2011**, *58*, 398-407.

[18] A. Otero-de-la-Roza, J. Mallory, E. Johnson, *Chem. Phys*, **2014**, *140*, 18A504.

[19] J. Ochterski, Ph. D. Gassian, **2000**, Inc. June 2.

[20] N.S. Babu, *Pelagia Research Library*, *Adv. Appl. Sci. Res.*, **2013**, *4*, 147-153.

[21] S.R. Whittleton, R.J. Boyd, T.B. Grindley, *J. Phys. Chem. A*, **2006**, *110*, 5893-5896.

[22] S.W. Benson, O. Dobis, *J. Phys. Chem. A*, **1998**, *102*, 5175-5181.

[23] H. Botti, M.N. T. Nauser, W.H. Koppenol, A. Denicola, R. Radi, Moller, D. Steinmann, *J. Phys. Chem. B*, **2010**, *114*, 16584-16593.

[24] L. Turker, *The ScientificWorld Journal*, **2012**, 2012.